Facile Synthesis of Silver Nanoparticles Using Asian Spider Flower and Its In Vitro Cytotoxic Activity Against Human Breast Carcinoma Cells

Authors:

Balashanmugam Pannerselvam, Prabhu Durai, Devasena Thiyagarajan, Hak Jin Song, Kwang Jin Kim, Yun Seok Jung, Hyung Joo Kim, Senthil Kumaran Rangarajulu

Date Submitted: 2020-06-10

Keywords: apoptotic protein-caspases, anticancer activity, breast cancer cell lines, cytotoxicity, silver nanoparticles, green biosynthesis

Abstract:

Cancer is one of the most dangerous threats to human health and possibly the utmost task for current medicine. Currently, bio-based synthesis of nanoparticles from plants has gained much interest due to its potential medicinal applications. In the present study, a biological approach was employed for biogenic (green) synthesis of silver nanoparticles (AgNPs) using dried leaf extract of Asian spider flower (Asf). The biogenic synthesis of Asf-AgNPs (Asian spider flower-Silver nanoparticles) was established using ultra violet-visible (UV-vis) spectra which exhibited a wide superficial plasmon resonance of AgNPs at 445 nm. These nanoparticles clearly showed the formation of poly-disperse crystalline solids (spherical shape) with particle size range of <50 nm based on observation under a transmission electron microscope (TEM). Infrared spectroscopy (FTIR) revealed carboxylic acids (C = O stretch) known to act as a capping agent and a reductant in plant extracts. Elemental silver signal peak was observed in the graph obtained from energy-dispersive X-ray (EDX) analysis. Biocompatibility tests for Asf-AgNPs at different doses were evaluated against human breast cancer cells (MCF7) for cell viability and apoptotic analysis. According to the evaluation, biosynthesized Asf-AgNPs could prevent the explosion of human breast tumor cells (MCF7) in IC50 at a dose of 40 ?g/mL after 48 h of treatment. The results obtained in the IC50 dosage treatments were statistically significant ($p < 0.05$) when compared with control. Nuclear damage of cells was further investigated using annexin V-FITC/PI dual staining and DAPI (4?,6-diamidino-2-phenylindole) staining method. Bright blue fluorescence with condensed and fragmented chromatin was observed. Western blot analysis showed increased expression levels of caspases-3 and 9 (apoptotic proteins). These results indicate that bio-approached AgNPs synthesized through Asf plant extract could be used as potential therapeutic medications for human cancer cells.

Record Type: Published Article

Submitted To: LAPSE (Living Archive for Process Systems Engineering)

Citation (overall record, always the latest version):	LAPSE:2020.0582
Citation (this specific file, latest version):	LAPSE:2020.0582-1
Citation (this specific file, this version):	LAPSE:2020.0582-1v1

DOI of Published Version: https://doi.org/10.3390/pr8040430

processes

MDPI

Article

Facile Synthesis of Silver Nanoparticles Using Asian Spider Flower and Its *In Vitro* Cytotoxic Activity Against Human Breast Carcinoma Cells

Balashanmugam Pannerselvam [1], Prabhu Durai [2], Devasena Thiyagarajan [1], Hak Jin Song [3], Kwang Jin Kim [4], Yun Seok Jung [5], Hyung Joo Kim [3] and Senthil Kumaran Rangarajulu [3,*]

1 Centre for Nanoscience and Technology, Anna University, Chennai, Tamil Nadu 600025, India; biobala17@gmail.com (B.P.); tdevasenabio@gmail.com (D.T.)
2 Department of Zoology, Government College of Arts & Science, Thennangur, Tamil Nadu 673018, India; prabhud1986@gmail.com
3 Department of Biological Engineering, Konkuk University, Seoul 05029, Korea; hjeda11@konkuk.ac.kr (H.J.S.); hyungkim@konkuk.ac.kr (H.J.K.)
4 Urban Agriculture Research Division, NIHHS, Wanjoo 54875, Korea; kwangjin@korea.kr
5 Department of Beauty & Cosmetology, Jeju National University, Jeju 63243, Korea; jbgroup@jejunu.ac.kr
* Correspondence: kumaran.ran@gmail.com or kumaran@konkuk.ac.kr; Tel.: +82-2-2049-6112

Received: 3 March 2020; Accepted: 30 March 2020; Published: 4 April 2020

Abstract: Cancer is one of the most dangerous threats to human health and possibly the utmost task for current medicine. Currently, bio-based synthesis of nanoparticles from plants has gained much interest due to its potential medicinal applications. In the present study, a biological approach was employed for biogenic (green) synthesis of silver nanoparticles (AgNPs) using dried leaf extract of Asian spider flower (Asf). The biogenic synthesis of Asf-AgNPs (Asian spider flower-Silver nanoparticles) was established using ultra violet-visible (UV-vis) spectra which exhibited a wide superficial plasmon resonance of AgNPs at 445 nm. These nanoparticles clearly showed the formation of poly-disperse crystalline solids (spherical shape) with particle size range of <50 nm based on observation under a transmission electron microscope (TEM). Infrared spectroscopy (FTIR) revealed carboxylic acids (C = O stretch) known to act as a capping agent and a reductant in plant extracts. Elemental silver signal peak was observed in the graph obtained from energy-dispersive X-ray (EDX) analysis. Biocompatibility tests for Asf-AgNPs at different doses were evaluated against human breast cancer cells (MCF7) for cell viability and apoptotic analysis. According to the evaluation, biosynthesized Asf-AgNPs could prevent the explosion of human breast tumor cells (MCF7) in IC_{50} at a dose of 40 µg/mL after 48 h of treatment. The results obtained in the IC_{50} dosage treatments were statistically significant ($p < 0.05$) when compared with control. Nuclear damage of cells was further investigated using annexin V-FITC/PI dual staining and DAPI (4′,6-diamidino-2-phenylindole) staining method. Bright blue fluorescence with condensed and fragmented chromatin was observed. Western blot analysis showed increased expression levels of caspases-3 and 9 (apoptotic proteins). These results indicate that bio-approached AgNPs synthesized through Asf plant extract could be used as potential therapeutic medications for human cancer cells.

Keywords: green biosynthesis; silver nanoparticles; cytotoxicity; breast cancer cell lines; anticancer activity; apoptotic protein-caspases

1. Introduction

Nanotechnology, a branch of technology for the production of nanoscale materials including graphite, carbon nanotubes, and fullerenes with sizes of 1 to 100 nm, has gained attention due to its

astonishing properties [1–4] for a wide range of applications in many arenas. Metallic nanoparticles exist in different categories such as gold, silver, alloy, zinc, and so on [5–7]. Nanotechnology has shown significance in fields of biology, medicine, and electronics due to distinctive particle sizes and shapes of nanoparticles and their physical, chemical, and biological properties [8]. The combination of oncology and nanotechnology has given birth to a novel and innovative field, known as neuronanomedicine, which incorporates various nanoformulations and nanomaterials in order to investigate pathological and carcinogenic mechanisms at the microscopic level for imaging, diagnosis and cancer treatment, including female specific-cancers such as breast cancer [9]. Breast cancer is the most common malignancy among women worldwide, and the highest number of cases is seen in developed countries like the U.S., with 1.67 million new cases diagnosed in the year 2014 [10,11]. Silver nanoparticles (AgNPs) possess distinctive properties including antimicrobial, non-toxic qualities, making them useful for medicine and consumer products [12]. AgNPs have been employed in various fields such as imaging, water and air purifiers, textiles, energy sector, sensors, antibacterial products, and anticancer agents [13–16]. Silver nanoparticles have unique optical properties that enable them to interact at a specific wavelength of light. They are even hybridized with other materials in order to enhance drug efficacy and signaling in multiple biosensing platforms [17].

Bio-based approaches for the synthesis of nanoparticles have gained abundant attention in biomedical investigation by developing novel and enhanced goods for health diagnosis in various therapies. Electronic or ionic interaction between chemical functional groups and metal composites in the biomass had led to the formation of biologically synthesized NPs. Concerned metal is further solubilized with a reducing agent, stabilizing agent, and a solvent for the synthesis of nanoparticles. Performances of a wide range of natural bioorganic compounds (viz. flavonoids, terpenoids, proteins, reducing sugars, and alkaloids) utilized as doping or plummeting agents have been evaluated [18]. Plant biomass can act as a plummeting agent, an alleviating agent, and a solvent that is cost-effective and ecofriendly [19]. Silver nanoparticles have diverse in vitro and in vivo applications due to their effective antimicrobial activities and low toxicities. In addition, AgNPs eased by herbal extracts have been demonstrated to be operative cytotoxic mediators [20,21].

Asian spider flower (Asf) or tick weed (Scientific name: *Cleome viscosa*) belonging to family Cleomaceae [22] is a yearly plant distributed in all parts of the world. It has been used as a remedial plant owing to its wide-ranging of biological welfares [23,24]. This plant has creamy flowers and pods that are lengthy and tubular. It has somewhat dark seeds [25]. It also contains a diverse range of therapeutic components with various pharmacological activities. It is nontoxic since its young buds and leaves can be used as a vegetable. In Ayurveda medication, the Asf is used as an anthelmintic [26] treatment. It is also used to treat pruritus and numerous illnesses such as gastrointestinal complaints, gastrointestinal diseases, etc. [27,28] in humans. It is also used as an herbal drug to treat ringworm, flatulence, colic, dyspepsia, cough, bronchitis, and cardiac illnesses. Leaves from the plant are used as an exterior application to treat inflammation of the middle ear [29], wounds, and ulcers [30]. They also have hepatoprotective principle [31] and can potentially be used in liver disease treatments. Traditionally, this plant is used to treat fever, inflammation, liver illnesses, bronchitis, skin illnesses, and malarial fever [32]. The juice of its leaves is applied to the skin as a counterirritant. Its roots are used as a remedy for scurvy and rheumatism [33,34]. Based on the literature about its bioactivities mentioned above, Asf could be a good candidate in the preparation of silver nanoparticles (AgNPs) to obtain pharmacological effects. In this work, we used a biological and ecofriendly approach to synthesize AgNPs incorporating with extracts of Asf leaves. These prepared AgNPs were characterized using different instruments. Their cytotoxic activity against human breast tumor (MCF7) cell line was also determined.

2. Results and Discussion

2.1. Biological Synthesis and Silver Nanoparticles Characterization

Plant extracts encompass numerous primary and secondary functional metabolites. They might effectively reduce silver ions to silver nanoparticles with stable condition. Plant extracts contain equally polar and nonpolar compounds that can improve nanoparticle synthesis. The procedure of reduction of an aqueous solution of silver nitrate is henceforth the most broadly used technique for the production of silver nano colloids [35]. In a previous study, a phytochemical screening of Asf extracts has revealed the presence of terpenes, flavonoids, phenol carboxylic acid, and polyphenols [36]. In this work, nanoparticles were manufactured by mixing Asf leaves extract (1 mL from stock) with 1 mM aqueous $AgNO_3$ solution for 2 h to form AgNPs (yellowish-brown precipitation) (Figure 1). In the colloidal solution of nanoparticles, alteration in color was observed owing to the excitation of superficial plasmon vibrations (fundamentally the vibration of the group leading electrons) [37]. Ultra violet-visible (UV-vis) absorption spectra at 445 nm showed a wide range of surface plasmon resonance. In vitro constancy of Asf-AgNPs (Asian spider flower-Silver nanoparticles) was examined by observing plasmon wavelength and plasmon bandwidth at different time points (12, 24, 48, 72, and 96 h) (Figure 2). As stated previously, the test was set up with variable intervals (viz., 5, 15, 25, 35, 45, 60, 90 min). Testers were then scanned in the range of 400–600 nm to notice the development of extensive absorbance peak and color alteration implication [38]. Similar observations reported earlier in viewing a stable upsurge in the strength of SPR without any alteration in peak location is demonstrated in the synthesis of AgNPs with *Carica papaya* latex at different reaction time (0 to 72 h) [39]. Additionally, in the same study, using *Euphorbia antiquorum* latex extract, SPR intensity is increased with a decrease of silver ions after 24 h of incubation at room temperature from manufactured AgNPs [40]. Moreover, UV–Vis investigation ascertained the formation of stable metal nanoparticles exhibiting novel optical properties [41]. Synthesis of Size-controlled nanoparticles for stable systems have been prepared through combined action of solvated metal atom dispersion technique [42].

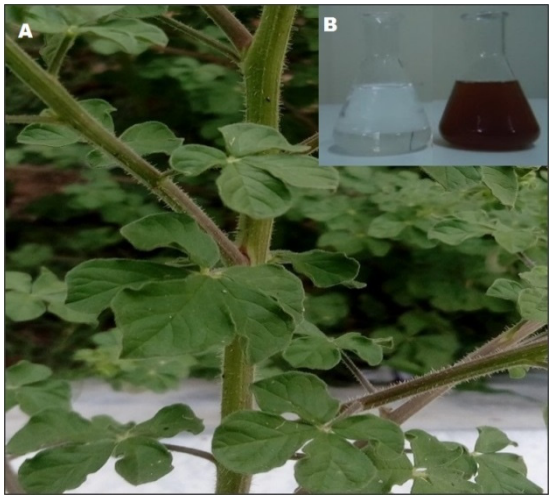

Figure 1. (**A**) Asian spider flower (*C. viscosa*) plant morphology, (**B**) Production of silver nanoparticles (AgNPs) with the development of a dark brown color designating a decrease of Ag+ into Ag^0.

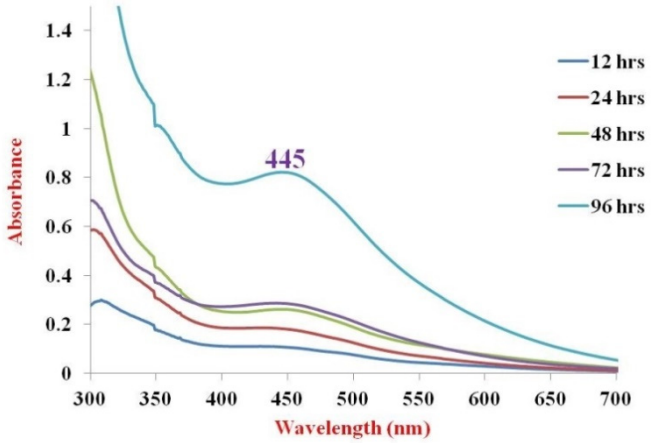

Figure 2. UV–Vis spectroscopy of intense SPR spectra at 445 nm. The maximum absorbance was noticed with increased incubation time (up to 96 hrs).

The size and morphology of prepared silver nanoparticles were analyzed using transmission electron microscopy (TEM) (Figure 3), which clearly exhibited the formation of polydisperse spherical and different magnitudes of crystalline AgNPs ranging from 20 to 50 nm in diameter, consistent with results of previous studies [43,44]. Elementary compositions of these biosynthesized silver nanoparticles were determined by energy-dispersive X-ray (EDX) spectrum analysis (Figure 4). Results showed a distinct signal at 0.2 and 3 KeV regions representing the development of AgNPs from the leaf extract of Asf. The spectrum also designates that peaks designed are owing to the occurrence of copper from carbon-coated copper grids. Likewise, the third extreme peak positioned on the spectrum at 3 KeV designates the attendance of elemental silver from manufactured silver nanoparticles arbitrated compound [34]. The information provided by the infrared spectroscopy (FTIR) spectra was able to recognize biomolecules accountable for plugging and stabilizing these silver nanoparticles. Treatments with the Asf extract showed intense peaks at 2996, 1750, 1375, 1250, 1065, 870, 671, and 481 cm^{-1}. These synthesized particles (Asf-AgNPs) showed bands at 2996, 1747, 1375, 1249, 1065, 862, and 6650 cm^{-1}, 1747 cm^{-1} (C = O stretch), 1375 cm^{-1} (N = O stretch), 1249 cm^{-1} (C-O stretch) (Figure 5). These results indicate that carboxylic acids present in the plant extract can act as a capping and reducing mediator for the development of functionalized AgNPs. Comparable explanations have also been suggested for silver nanoparticles synthesized with *Desmodium gangeticum* [45]. The action of plugging and stabilization on AgNPs brings a well-organized biosynthesis technique with less toxicity [46–48]. To determine the size distribution of synthesized Asf-AgNPs, dynamic light scattering of particles was measured. Figure 6A showed the size distribution of particles with a maximum intensity at 19.59 nm. Figure 6B showed the zeta potential of stable dispersion of AgNPs at 8.30 mV. Such green synthesized particles showed good stability and well dispersibility mainly due to the presence of plant based functional metabolites known to have less toxic effects on human cells [49,50]. Green manufactured silver nanoparticles using *Oscillatoria limnetica* aqueous extract has known to act as a dipping and stabilizing agent have also been reported [51].

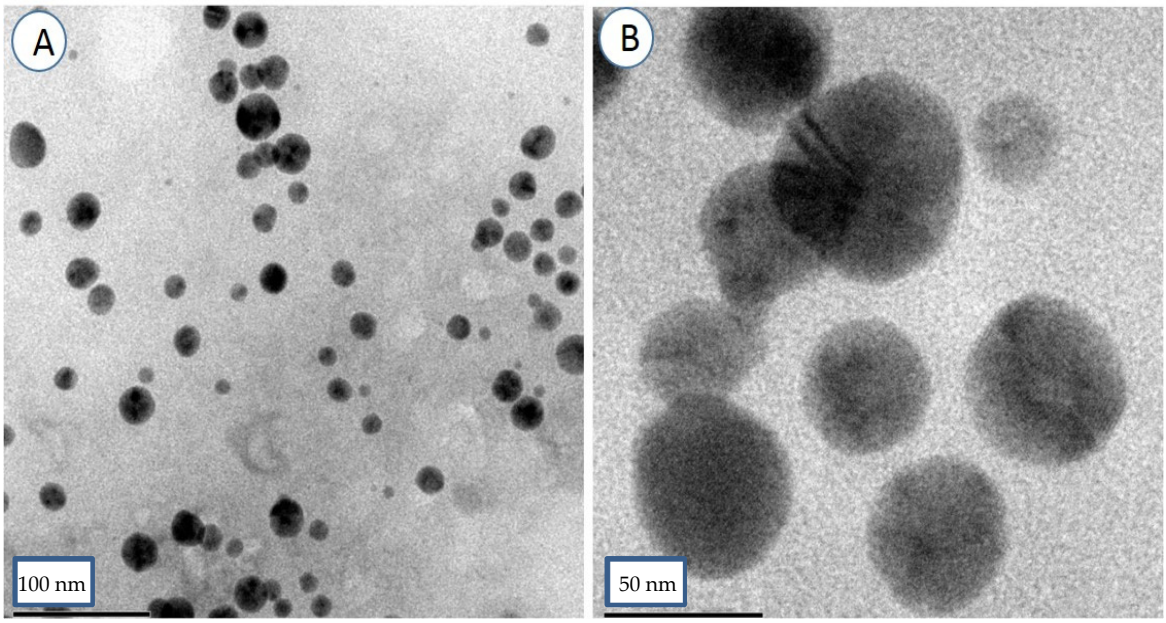

Figure 3. (**A**) and (**B**) transmission electron microscope (TEM) images of AgNPs manufactured from Asian spider flower (Asf)-leaves, showing different particle size.

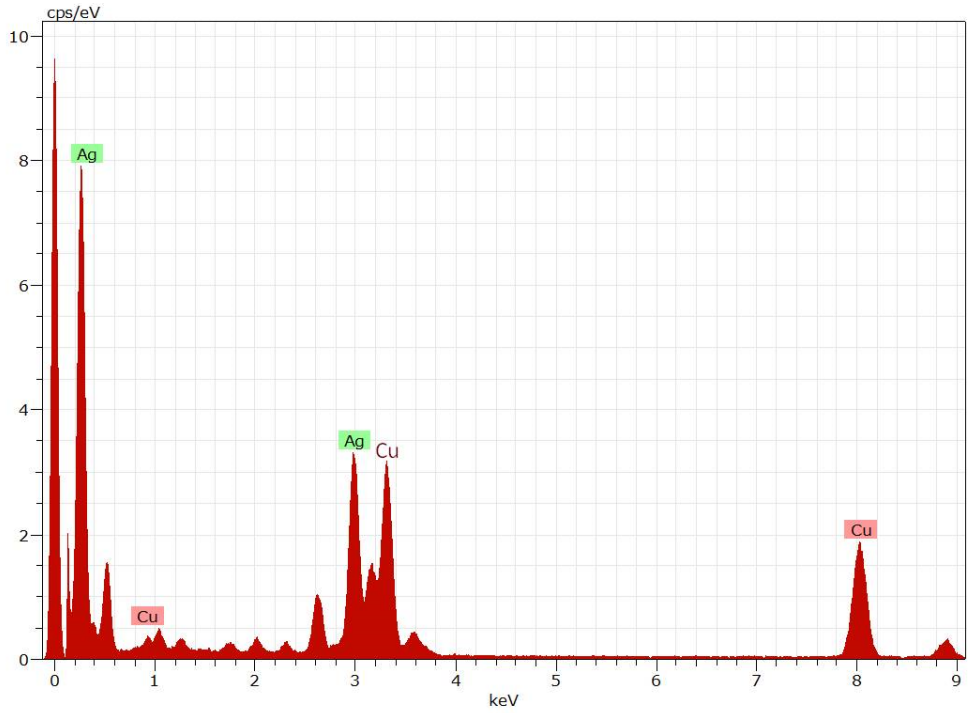

Figure 4. Energy-dispersive X-ray (EDX) analysis showing a strong peak of silver from synthesized Asf-AgNPs.

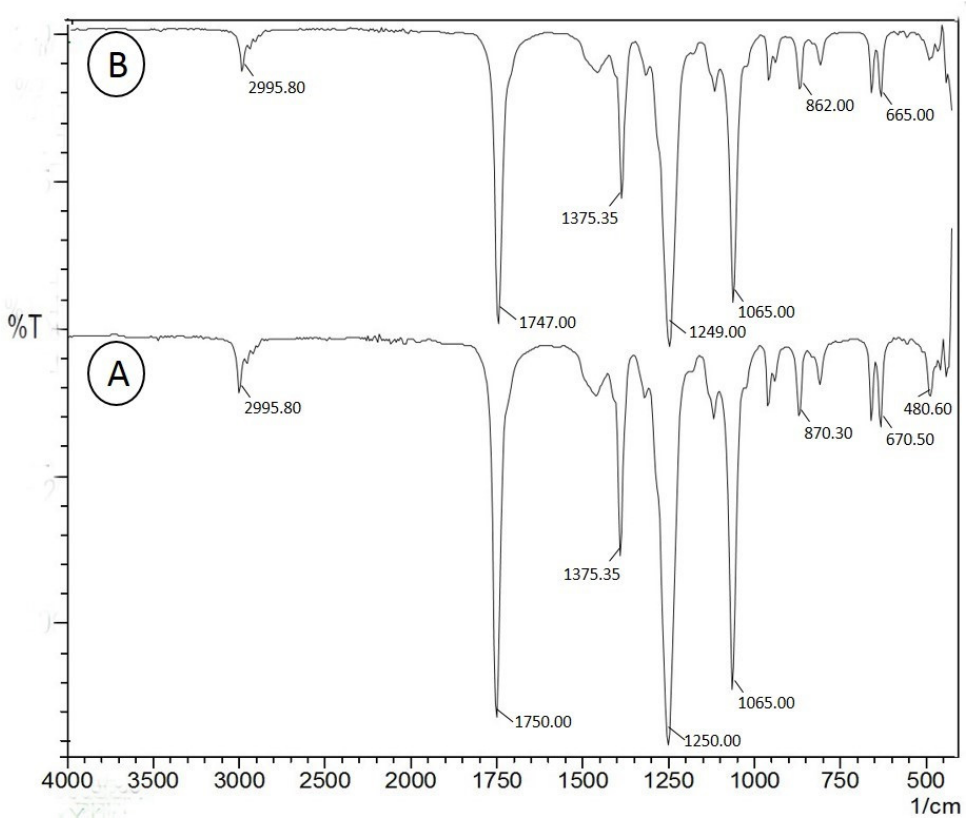

Figure 5. FT-IR spectra of Asian spider flower (Asf) plant extract (**A**) and AgNPs manufactured from Asf (**B**).

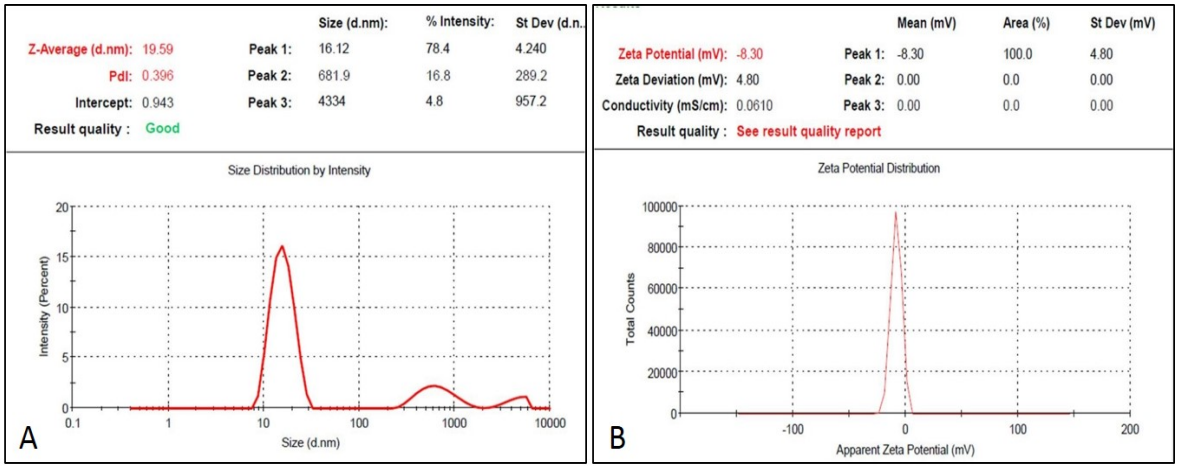

Figure 6. Dynamic light scattering (DLS) profile. (**A**) Size distribution of Asf-AgNPs (Asian spider flower-Silver nanoparticles) with maximum intensity at 19.59 nm, (**B**) Stable Asf-AgNPs at −8.30 Mv in zeta potential analysis.

2.2. MTT (3-(4,5-dimethylthiazol-2-yl)-2,5-diphenyltetrazolium bromide) Assay

The present investigation the inhibitory effects of different concentrations (5, 10, 20, 40, 80, and 160 µg/mL) of silver nitrate ($AgNO_3$) and synthesized Asf-AgNPs under in vitro conditions on MCF7 breast cancer cell line and normal green monkey kidney cell line was determined using MTT (3-(4,5-dimethylthiazol-2-yl)-2,5-diphenyltetrazolium bromide) test (Figures 7 and 8). MCF7 cells preserved through silver nanoparticles (40 µg/mL) after 48 h of development with 50% hang-up of cell propagation. In contrast, while the same concentrations of Asf-AgNPs were used to treat normal Vero

cells, showing the inhibition of cell viability was observed only at maximum concentrations (85.77% inhibition after 48 h incubation). The activity of Asf-AgNPs on Vero cell line was constantly less at experimented dilutions as compared with cancer cell line. Furthermore, in the same concentration of $AgNO_3$ were used to both MCF7 and Vero cells showed highly significant ($p < 0.05$) reduce the cell viability when compared to the control. The cell viability assay made in the present attempt indicated that synthesized Asf-AgNPs are less toxic than $AgNO_3$ and the biocompatibility of Asf-AgNPs was gradually increased at all concentrations by dose and time dependent. *C. viscosa* extract mediated AgNPs and $AgNO_3$ alone used to treated and untreated MCF7 and Vero cells at 48 hrs were observed under inverted microscope. Figure 9A,D untreated (control) Vero and MCF7 showed irregular confluent aggregates with round polygonal cells appeared normal. Figure 9B,E showed $AgNO_3$ treated Vero and MCF7 cells appeared to have shrinkage, become spherical in shape, and detached dead cells. In contrast, Vero and MCF7 cells treated with AgNPs shows persuade cell reduction lead to the changes in membrane integrity and cell shrinkage due to physiognomies of apoptotic cell demise (Figure 9C,F). These results were similar to previous reports [52,53], which was mainly based on the agents that cause reduction and capping silver nitrate into silver. Cell uptake and internalization of nanomaterials are key factors determined by the surface property of AgNPs [54]. This permeabilization activity is based on surface charges of AgNPs and cell membranes [55–58]. Based on the results of inhibitory activity and cell morphology observation, the IC_{50} concentration of Asf-AgNPs and control alone were used for further apoptotic experiments.

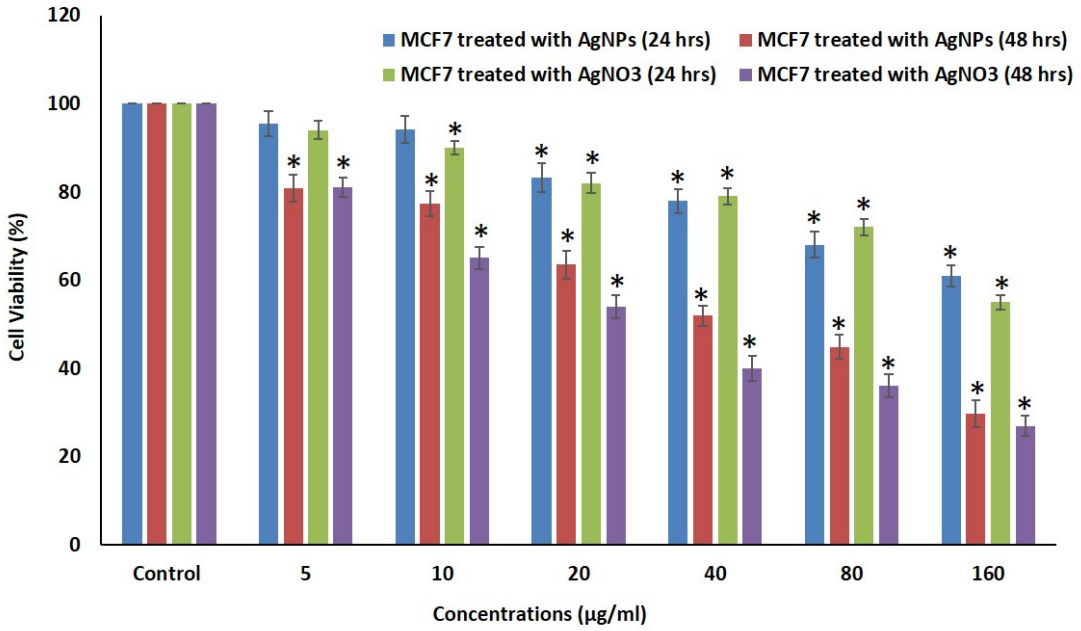

Figure 7. Inhibitory outcome of $AgNO_3$ and AgNPs manufactured from leaves extract of Asf on MCF7 cells at 24 and 48 hrs. Values are given as mean ± S.D. for each concentration. *Indicates the treated concentrations statistically significant ($p < 0.05$) when compared to control.

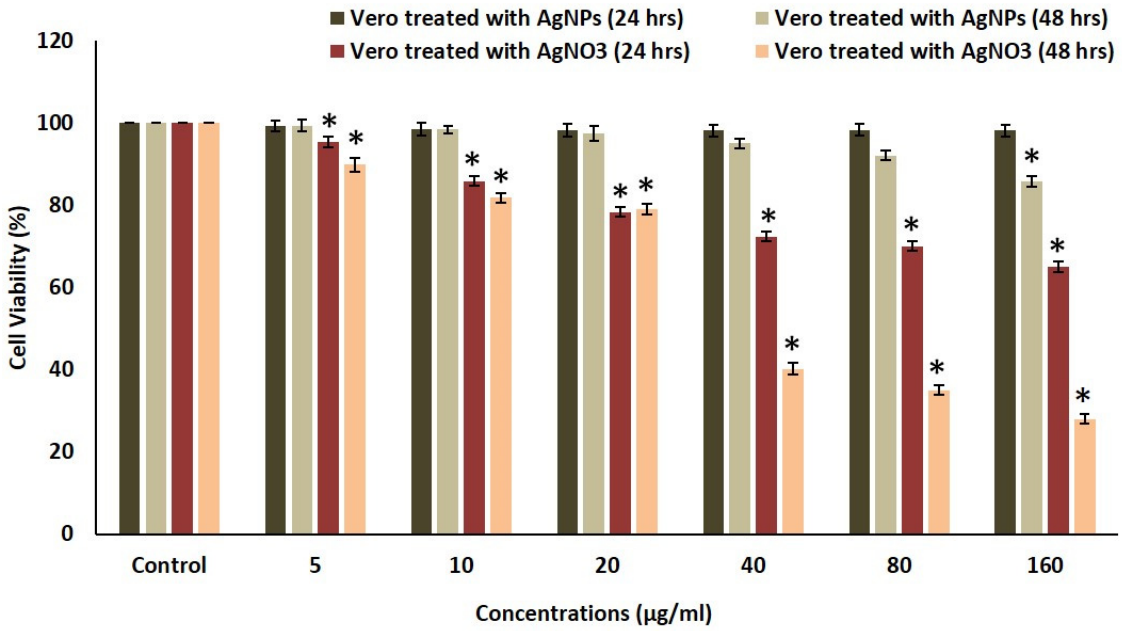

Figure 8. Effect of $AgNO_3$ and Asf-AgNPs on normal Vero cells at 24 and 48 hrs. Values are given as mean ± S.D. for each concentration. *Indicates the treated concentrations statistically significant ($p < 0.05$) when compared to control.

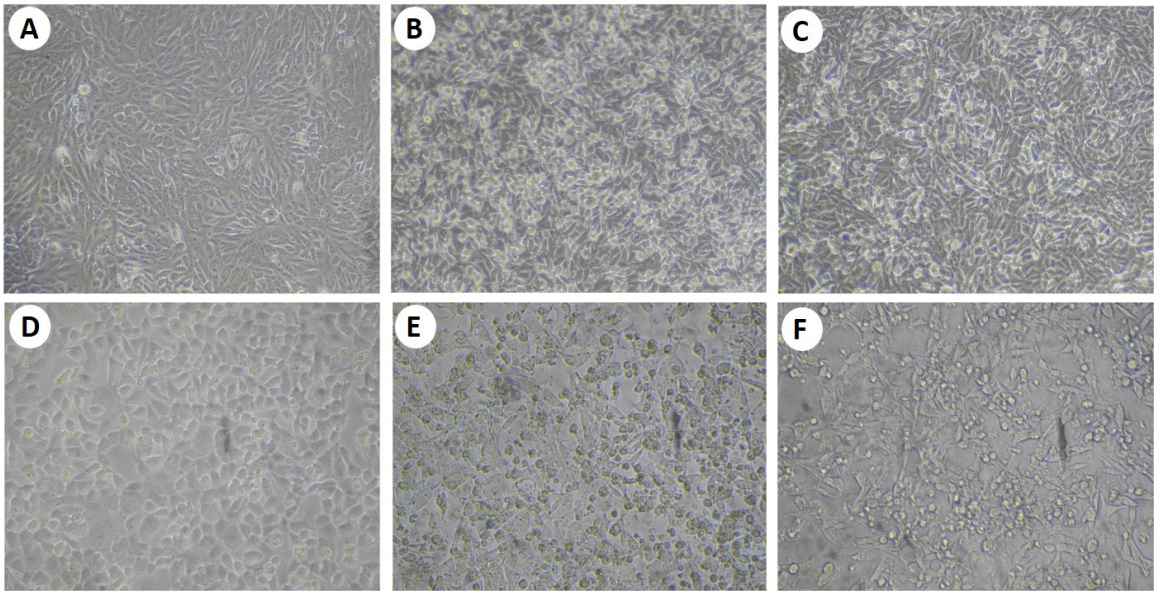

Figure 9. Effect of $AgNO_3$ and Asf-AgNPs on cell morphology of MCF7 and Vero cell line at 48 h. (**A**) Control (Vero), (**B**) $AgNO_3$ treated on Vero (40 µg/mL), (**C**) Asf-AgNPs treated on Vero (40 µg/mL), (**D**) Control (MCF7), (**E**) $AgNO_3$ treated on MCF7 (40 µg/mL), (**F**) Asf-AgNPs treated on MCF7 (IC_{50} – 40 µg/mL).

2.3. Apoptosis Study

In bio-cellular systems, cell death (apoptosis or involuntary cell demise) is a well-documented spectacle that has been clearly witnessed. Experimental topographies of apoptosis comprise the following: reduced cell extent and chromatin reduction, and nuclear disintegration owing to endonuclease breaking of DNA. Membrane phospholipid phosphatidylserine (PS) is changing location from internal to the external leaflet of plasma membrane in the initial stage of cell demise,

revealing PS to the outside of cellular atmosphere. Annexin V is a 35–36 kDa calcium-dependent phospholipid-required protein connected with a high empathy for PS. It binds to unprotected apoptotic cell's superficial PS to facilitate the initial of apoptosis. The PI is a red glowing dye that enters a cell depending on the penetrability of the membrane [30]. Results of annexin V-FITC/PI dual staining are shown in Figure 10A,B. The control cells of MCF7 showed negative staining in reaction with annexin V-FITC and PI. However, MCF7 cells treated with Asf extract arbitrated AgNPs at IC_{50} (40 µg/mL) showed positive staining with annexin V and PI, which lead the indication sign on the progress of apoptosis. The apoptotic effect of Asf-AgNPs on MCF7 cells was observed through DAPI (4′,6-diamidino-2-phenylindole) staining (Figure 11). DAPI is a nuclear stain that stains injured DNA in the central nucleus. The contact of AgNPs with MCF7 cancer cells produced a bright blue fluorescence with shortened and disjointed chromatin compared to less effective fluorescence for control cells (untreated). Earlier reports have suggested that plant formulated syntheses of AgNPs are responsible for the generation of oxidative stress, caspase dependent apoptosis, and mitochondrial dysfunction [59]. The cytotoxic effect of AgNPs formulated from the extracts of *Kleinia grandiflora* [60] or *Punica granatum* on DNA damage in cancer cells also provides evidence that such NPs might have anticancer activities [61].

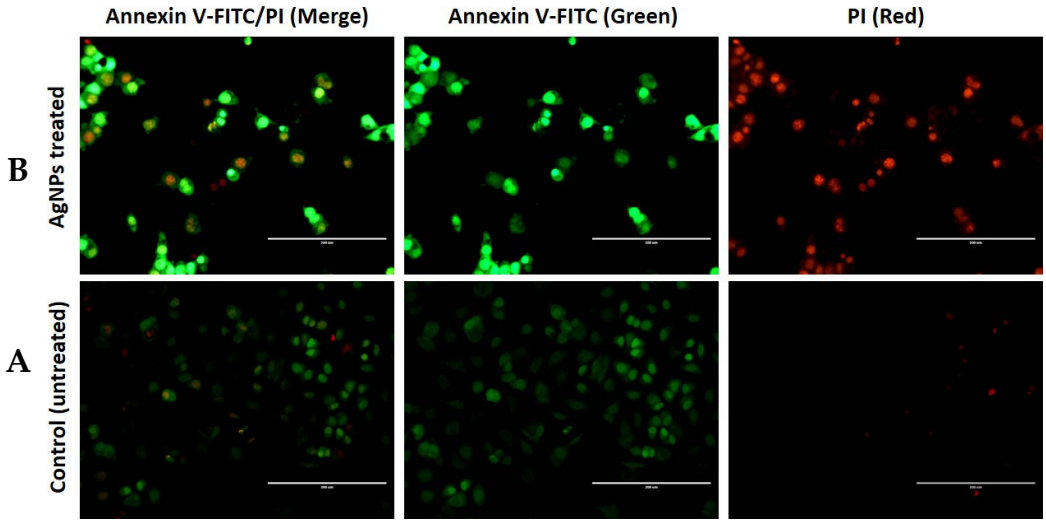

Figure 10. Manufactured Asf-AgNPs induced apoptosis of MCF7 cells as established through phosphatidylserine translocation using a fluorescent microscope. Control cells displayed no Annexin V-FITC/PI staining (**A**). Cells treated with Asf-AgNPs (IC_{50} 40 µg/mL at 48 h) showed double staining of Annexin V-FITC/PI, indicating apoptosis (**B**).

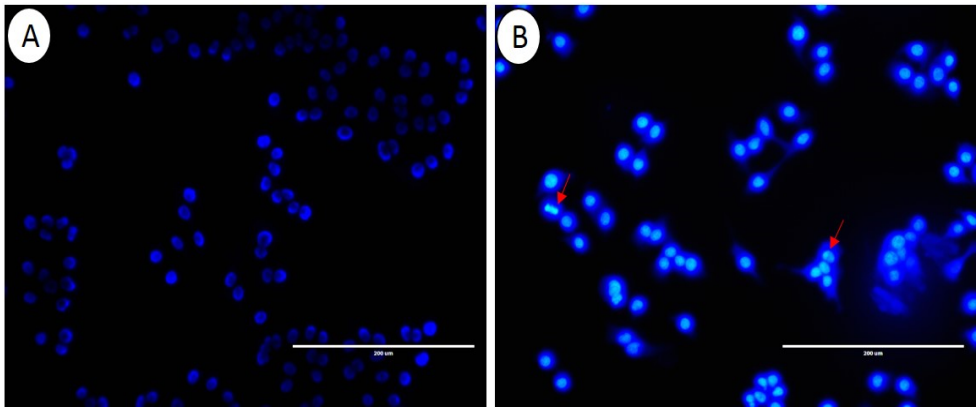

Figure 11. DAPI (4′,6-diamidino-2-phenylindole) pictures of MCF7 cells. Control cells (**A**), Cells treated with Asf-AgNPs. (**B**). Red arrows designate apoptotic cells.

2.4. Western Blot Investigation

The maintenance of homeostasis through the regulation of cell death and inflammation is governed by a family of caspases. Caspase stimulation is generally considered to be an important marker of apoptosis led by several apoptotic mediators [62]. Among them, cysteine proteases serve as primary mediators of apoptosis. In the mammalian system, apoptotic caspase-3 is not an initiator caspase but acts an executioner which leads to the degradation of cellular components for apoptosis. In general it has three functional groups: caspases 3, 8, and 9. Involuntary cell death is commenced by the stimulation of caspase cascade (caspases 3, 6, and 9) followed by the capture of G2/M phase in the cell cycle [63]. Caspase-3 is an important killer of apoptosis. Its active form is vital for flouting cellular modules associated with DNA overhaul and regulation. Caspase-3 has also been used in numerous circumstances such as for anticancer drug handling [64]. In this work, MCF7 cells treated with Asf-AgNPs triggered apoptosis showing an up-regulation on the active forms of caspases 3 and 9 (Figure 12). MCF7 cells treated with Asf-AgNPs showed enhanced expression levels of caspases-3 and 9 compared to MCF7 cells without Asf-AgNPs. B-actin was used as an internal control. The statistical significance in the in the over expression of apoptotic protein was observed in the treatments (MCF7 treated with Asf-AgNPs (IC_{50} at 40 µg/mL) when compared with the control at p value < 0.05. Manikandan et al. [65] have reported that *Solanum trilobatum* extract can decide the AgNPs-influenced ROS generation and trigger the inherent apoptotic pathway. Modulation of anti-apoptotic (Bax and Bcl-2) and apoptotic (caspase-3 and 9) protein countenance in mitochondria can affect cell death through a caspase-dependent pathway. Previous reports have revealed that AgNPs have shown acceptable potential anticancer activities [66–69] in human cancer.

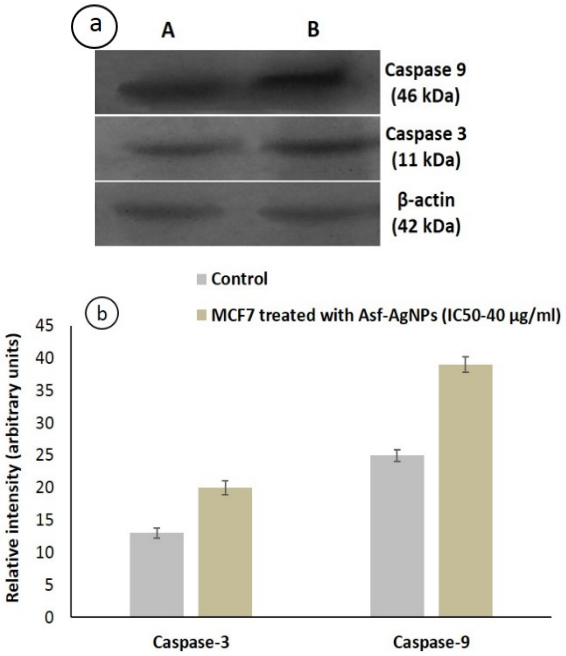

Figure 12. (**a**) Effects of Asf-AgNPs on expression levels of caspases 3 and 9 apoptotic proteins by western blot analysis. (A) Control, (B) Asf-AgNPs (IC_{50} concentration at 40 µg/mL with 48 h). (**b**) Quantitative data representing the corresponding protein levels assessed using densitometry. Y axis represents relative intensity (arbitrary units). Each column represents the mean ± SD of three independently performed experiments. The statistical significance in the expression of apoptotic protein was observed in the treatments (MCF7 treated with Asf-AgNPs (IC_{50} at 40 µg/mL) when compared with the control at p value < 0.05.

3. Materials and Methods

3.1. Plant Selection and Extract Preparation

Asian spider flower (Asf) (*Cleome viscosa* L.) was collected, identified, and authenticated by botanists. Leaves of the Asf were dehydrated under a shade condition at 30 °C and then milled to powder. The powder sample (5 g) was then heated in 100 mL of distilled water for 20 min and clarified thrice using a Whatman number 1 sieve paper. The filtrate was stored at 4 °C in a refrigerator until analysis.

3.2. Silver Nanoparticles Synthesis

Silver nitrate (1 mM) aqueous solution was utilized to produce nano silver. To 45 mL of silver nitrate solution (1 mM), 5 mL of Asf extract was added and mixed. The mixture was then incubated at 30 °C in the dark for 12 h to reduce silver nitrate to silver ions.

3.3. Characterization of Silver Nanoparticles

The bio-reduction of sliver nitrates to ions of silver was observed with a UV-Visible spectrophotometer (Shimadzu-1800, Kyoto, Japan). Measurements were performed at room temperature using silver nitrate (1 mM) as a blank at wavelength of 300 to 700 nm with a resolution of 1 nm. These synthesized nanoparticles were then analyzed with a transmission electron microscope (TEM, FEI, TECNAI T30). The TEM samples were prepared by dropping aqueous dispersions onto carbon-coated copper grids and then dehydrated it at 30 °C. Various sizes of NPs obtained from a random field of TEM images were measured for determination of general morphology of nanoparticles. The biomolecules associated with the NPs were further identified using Fourier Transform Infrared (FTIR) spectroscopy (Perkin-Elmer, Waltham, MA, USA) with diffuse reflectance method at a resolution of 4 cm^{-1} in KBr pellets. Element compositions of nanoparticles were determined with Energy Dispersive X-ray Spectroscopy (EDX) analysis. Particle size and zeta potential were measured with a Malvern Zetasizer Nano ZS (Malvern Instruments Ltd., Malvern, UK).

3.4. Cell Culture and Maintenance

Breast cancer cell lines (MCF-7) were tested in this investigation. These cells were cultured with DMEM (Dulbecco's Modified Eagle Media) medium supplemented with fetal bovine serum (FBS) (10%) and penicillin/streptomycin (1%). Cells were cultured at 37 °C with 5% CO_2 water-saturated atmosphere. For further investigation, cells passaged at pre-confluent concentrations were used.

3.5. Analysis of Cell Viability

MTT dye uptake method [70] was adopted to determine cell viability. DMEM added with L-glutamine (2 mM), penicillin (100 U/mL), streptomycin (100 µg/mL), FBS (10%) was used as a carbon source for MCF-7 cell line. Cell culture flasks of 25 cm^2 were incubated at 37 °C in 5% CO_2 atmosphere. For further dosage studies, cells were seeded into 96-well plates (1×10^6 cells in each well) and incubated at 37 °C for 24 h. MCF 7 breast cancer cells and normal Vero cells were treated with Asf-AgNPs and $AgNO_3$ alone at various dosages (5, 10, 20, 40, 80, and 160 µg/mL). Plates were incubated for 24 and 48 h with additional treatment followed by cell viability test using 3-(4,5-dimethylthiazol-2-yl)-2,5-diphenyltetrazolium bromide (MTT). After MTT solution (10 µL) was added to each well at concentration of 5 mg/mL, plates were incubated at 37 °C for 4 h. Formazan crystals of purple color appeared were dissolved in 100 µL of dimethyl sulfoxide (DMSO). Using a multi-well ELISA plate reader, the optical density was measured at 570 nm. With the following method, the % of cell viability was calculated.

$$\% \text{ of cell viability} = \text{OD of Sample/OD of Control} \times 100$$

3.6. Morphological Analysis

In 6-well plates, MCF7 and Vero cells (1×10^5) were treated with IC_{50} concentrations of Asf-AgNPs (40 µg/mL) at 48 hrs and $AgNO_3$ (40 µg/mL) at 48 hrs along with control (untreated). Further, the plates were washed twice with phosphate-buffered saline (PBS) and the cell morphology was observed using a radical inverted microscope along with a camera.

3.7. Apoptosis Assay

Apoptotic cells were determined with a dual staining method following the manufacturer's protocol [71]. Cells (1×10^6/well) were cultured in 6-well plates and allowed to attach overnight with Asf-AgNPs (40 µg/mL) The IC_{50} concentrations also observed with the overnight treatment. Control cells were also maintained independently for 48 h. These cells were then collected, washed twice with PBS, and resuspended in 1x binding buffer (500 µL). Cells were then stained with annexin V-FITC conjugate (5 µL) and propidium iodide (PI) solution (10 µL) in dark at 30 °C for 15 min. Using a fluorescent microscope (EVOS® FLoid® Cell Imaging Station), stained cells were analyzed to determine the cell viability (with annexin V-FITC and PI negative) and also to detect the early apoptosis (with annexin V-FITC positive and PI negative), or late apoptosis (with annexin V-FITC and PI positive). The % of annexin V positive cells was used to quantify the degree of apoptosis after treatments.

3.8. DAPI (4',6-diamidino-2-phenylindole) Staining

The MCF-7 cells (1×10^6 cells/well) were cultured in nutrient media with the treatment of Asf-AgNPs and incubated at 37 °C for 48 h. Cells of control and treatment groups were washed twice with PBS. They were then fixed with paraformaldehyde (3.7%) at 30 °C for 15 min. After washing with PBS twice, they were then stained with 4', 6-diamidino-2-phenylindole (DAPI) solution for 10 min at 30 °C. Using a fluorescent microscope (EVOS® FLoid® Cell Imaging Station), cells were subsequently examined.

3.9. Western Blot Analysis

Six-well dishes were used for MCF 7 cell were culture and then treated with Asf-AgNPs 48 h. Control cells were also maintained for 48 h. Cells were harvested using buffer containing Tris-HCl (50 mM, pH 8.0), NaCl (150 mm), sodium azide (0.02%), phenylmethanesulfonyl fluoride, aprotinin, and Triton X (1%). Cell lysates were then centrifuged (12,000× *g* for 30 min at 4 °C) to harvest the supernatant as protein sample. Electrophoresis was performed for protein samples obtained from control and treated cell lines using 12% SDS-PAGE gel slabs. Protein bands obtained in the gel was transferred onto a nitrocellulose membrane. Immunoblotting was then carried out using primary antibodies against caspase 9 (mouse monoclonal antibody), caspase 3 (mouse monoclonal antibody), β-actin (mouse monoclonal antibody) at the manufacturer's recommended dilution after blocking with non-fat dry milk powder. Later, the membrane was incubated with mouse anti-goat peroxidase-tagged antibodies. Immune complexes were then detected using DAB (0.01%) and H_2O_2. The blot was further analyzed with the densitometry method of quantitation.

4. Conclusions

In this investigation, a biological approach was employed for the green synthesis of nanosilver particles (AgNPs) using dried leaves extract of Asian spider flower (Asf). The green chemistry approach in the synthesis AgNPs using plant extract was shown to be a simple, economical, efficient, and eco-friendly approach for medicinal applications. Asf leaves could be developed as promising bio-reductants to formulate functionalized silver nanoparticles. Formulated AgNPs were characterized through various spectral and microscopic analyses that clearly indicated the shape and size of crystalline nanoparticles. Such simple, rapid, and stable bio-based production of nanosilver nanoparticles displayed potential inhibitory cytotoxic effects on human breast carcinoma cells (MCF7). The Asf-AgNPs

treatments exhibiting the up-regulation in the production of caspases 3 and 9 (apoptotic proteins), which trigger the apoptotic pathway and cause significant cell demise. The poly-potential activity of green synthesized AgNPs was due to their specific morphological (shape and size) features that enabled easy permeation into cells for targeted therapy. Our present investigation provides a green synthesis approach for the production of AgNPs in an ecofriendly environment, and also displays its potential applications in anticancer therapy.

Author Contributions: Conceptualization, reviewing and editing, S.K.R.; investigation, writing—original draft, methodology, supervision B.P., D.T.; formal analysis, P.D.; resources, K.J.K.; data curation, H.J.S.; supervision, H.J.K.; project administration, Y.S.J. All authors have read and agreed to the published version of the manuscript.

Funding: This study was supported by R&D Program for Forest Science Technology (Project No. 2019157B10-1921-0101) funded by Korea Forest Service (Korea Forestry Promotion Institute), Rural Development Administration, Korea.

Conflicts of Interest: The authors declare no conflict of interest.

Abbreviations

Asf	Asian spider flower
AgNPs	Silver Nanoparticles
Asf-AgNPs	Asian spider flower- Silver Nanoparticles (formulated nanoparticles)
UV-vis	Ultra Violet-visible
FTIR	Fourier Transform Infrared Spectroscopy
TEM	Transmission Electron Microscopy
EDX	Energy Disperse X-ray
MCF7	Human Breast Cancer Cells
DMEM	Dulbecco's Modified Eagle Media
FBS	Fetal Bovine Serum
CO_2	Carbon dioxide
MTT	3-(4,5-dimethylthiazol-2-yl)-2,5-diphenyltetrazolium bromide
DMSO	Dimethyl sulfoxide
PBS	Phosphate-buffered saline
ELISA	Enzyme-Linked Immunosorbent Assay
OD	Optical Density
µg	Microgram
ml	Milligram
h	Hours
IC_{50}	The Half Maximal Inhibitory Concentration
FITC	Fluorescein Isothiocyanate
PI	Propidium Iodide
DAPI	(4′,6-diamidino-2-phenylindole)
G2/M	Growth 2/Mitosis

References

1. Zarina, A.; Nanda, A. Combined efficacy of antibiotics and biosynthesized silver nanoparticles from *Streptomyces albaduncus*. *Int. J. Pharm. Technol. Res.* **2014**, *6*, 1862–1869.
2. Zarina, A.; Nanda, A. Green approach for synthesis of silver nanoparticles from marine Streptomyces- MS 26 and their antibiotic efficacy. *J. Pharm. Sci. Res.* **2014**, *6*, 321–327.
3. Jafari, A.; Pourakbar, L.; Farhadi, K.; Mohamadgolizad, L.; Goosta, Y. Biological synthesis of silver nanoparticles and evaluation of antibacterial and antifungal properties of silver and copper nanoparticles. *Turk. J. Biol.* **2015**, *39*, 556–561. [CrossRef]
4. Jiang, B.; Li, C.; Dag, O.; Abe, H.; Takei, T.; Imai, T.; Hossain, S.A.; Islam, T.; Wood, K.; Henzie, J.; et al. Mesoporous metallic rhodium nanoparticles. *Nat. Commun.* **2017**, *8*, 15581. [CrossRef]

5. Singh, D.; Rathod, V.; Fatima, L.; Kausar, A.; Vidyashree, N.A.; Priyanka., B. Biologically reduced silver nanoparticles from Streptomyces sp. VDP-5 and its antibacterial efficacy. *Int. J. Pharm. Pharm. Sci. Res.* **2014**, *4*, 31–36.
6. Singh, D.; Rathod, V.; Ninganagouda, S.; Hiremath, J.; Singh, A.K.; Mathew, J. Optimization and characterization of silver nanoparticle by endophytic fungi Penicillium sp. Isolated from *Curcuma longa* (Turmeric) and application studies against MDR *E. coli* and *S. aureus*. *Bioinorg. Chem. Appl.* **2014**, *2014*, 408021. [CrossRef]
7. Bhosale, R.S.; Hajare, K.Y.; Mulay, B.; Mujumdar, S.; Kothawade, M. Biosynthesis, characterization and study of antimicrobial effect of silver nanoparticles by Actinomycetes spp. *Int. J. Curr. Microbiol. Appl. Sci.* **2015**, *2*, 144–151.
8. Mahdieh, M.; Zolanvari, A.; Azimee, A.S.; Mahdieh, M. Green biosynthesis of silver nanoparticles by *Spirulina Platensis*. *Sci. Iran.* **2012**, *19*, 926–929. [CrossRef]
9. Rajitha, B.; Malla, R.R.; Vadde, R.; Kasa, P.; Prasad, G.L.V.; Farran, B.; Kumari, S.; Pavitra, E.; Kamal, M.A.; Raju, G.S.R.; et al. Horizons of nanotechnology applications in female specific cancers. *Semin Cancer Biol.* **2019**, in press. [CrossRef]
10. Siegel, R.L.; Miller, K.D.; Jemal, A. Cancer statistics. *CA Cancer J. Clin.* **2015**, *65*, 5–29. [CrossRef]
11. Nagaraju, G.P.; Rajitha, B.; Aliya, S.; Kotipatruni, R.P.; Madanraj, A.S.; Hammond, A.; Park, D.; Chigurupati, S.; Alam, A.; Pattnaik, S. The role of adiponectin in obesity-associated female-specific carcinogenesis. *Cytokine Growth Factor Rev.* **2016**, *31*, 37–48. [CrossRef] [PubMed]
12. Henglein, A. Small particles research: Physicochemical properties of extremely small colloidal metal and semiconductor particles. *Chem. Rev.* **1989**, *89*, 1861–1873. [CrossRef]
13. Marambio-Jones, C.; Hoek, E.M.V. A review of the antibacterial effects of silver nanomaterials and potential implications for human health and the environment. *J. Nanopart. Res.* **2010**, *12*, 1531–1551. [CrossRef]
14. Malabadi, R.B.; Chalannavar, R.K.; Meti, N.T.; Mulgund, G.S.; Nataraja, K.; Vijaya Kumar, S. Synthesis of antimicrobial silver nanoparticles by callus cultures and in vitro derived plants of *Catharanthus roseus*. *Res. Pharm.* **2012**, *2*, 18–31.
15. Mittal, A.K.; Chisti, Y.; Banerjee, U.C. Synthesis of metallic nanoparticles using plant extracts. *Biotechnol. Adv.* **2013**, *3*, 346–356. [CrossRef]
16. Sankar, R.; Karthik, A.; Prabu, A.; Karthik, S.; Shivashangari, K.S.; Ravikumar, V. *Origanum vulgare* mediated biosynthesis of silver nanoparticles for its antibacterial and anticancer activity. *Colloid Surf. B.* **2013**, *108*, 80–84. [CrossRef]
17. Ganji Seeta, R.R.; Begum, D.; Sathish Kumar, M.; Gayathri, C.; Sung-Min, K.; Ishaq, N.K.; Pinninti Santosh, S.; Ganji Purnachandra, N.; Eluri, P.; Young-Kyu, H. Nanomaterials multifunctional behavior for enlightened cancer therapeutics. *Semin. Cancer Biol.* **2019**, in press. [CrossRef]
18. Zhou, Y.; Lin, W.; Huang, J.; Wang, W.; Gao, Y.; Lin, L.; Li, Q.; Lin, L.; Du, M. Biosynthesis of gold nanoparticles by foliar broths: Roles of biocompounds and other attributes of the extracts. *Nanoscale Res. Lett.* **2010**, *5*, 1351–1359. [CrossRef]
19. Singh, A.; Jain, D.; Upadhyay, M.K.; Khandelwal, N.; Verma, H.N. Green synthesis of silver nanoparticles using *Argemone mexicana* leaf extract and evaluation of their antimicrobial activities. *Dig. J. Nanomater. Biostruct.* **2010**, *5*, 483–489.
20. Seralathan, J.; Stevenson, P.; Subramaniam, S.; Raghavan, R.; Pemaiah, B.; Sivasubramanian, A.; Veerappan, A. Spectroscopy investigation on chemo-catalytic, free radical scavenging and bactericidal properties of biogenic silver nanoparticles synthesized using *Salicornia brachiata* aqueous extract. *Spectrochim. Acta A* **2014**, *118*, 349–355. [CrossRef]
21. Ahmed, K.B.A.; Subramanian, S.; Sivasubramanian, A.; Veerappan, G.; Veerappan, A. Preparation of gold nanoparticles using *Salicornia brachiata* plant extract and evaluation of catalytic and antibacterial activity. *Spectrochim. Acta A* **2014**, *130*, 54–58. [CrossRef] [PubMed]
22. Edeoga, H.O.; Omosun, G.; Osuagwu, G.G.E.; Mbaebie, B.O.; Madu, B.A. Micro morphological characters of the vegetative and floral organs of some cleome species from nigeria. *Am. Eurasian J. Sci. Res.* **2009**, *4*, 124–127.
23. Chandra, G.P.; Rao Ch, V. Pharamcognostical studies of *Cleome viscosa* linn. *IJNPR* **2012**, *3*, 527–534.
24. Upadhyay, R.K. *Cleome viscosa* Linn: A natural source of pharmaceuticals and pesticides. *Int. J. Green Pharm.* **2015**, *9*, 71–85. [CrossRef]

25. Anburaj, J.; Singh, C.R.; Sundarraj, S.; Kannan, S. In vitro regeneration of *Cleome viscosa* an important medicinal herb. *J. Cell Mol. Biol.* **2011**, *9*, 37–44.
26. Chandak, R.R.; Bhairat, K.N.; Devdhe, S.J.; Majmudar, H.F. In vitro evaluation of anthelmintic potential of leaves of *Cleome viscosa* linn. *Int. J. Pharm. Sci. Rev. Res.* **2010**, *5*, 77–79.
27. Parimala Devi, B.; Boominathan, R.; Mandal, S.C. Evaluation of antidiarrheal activity of *Cleome viscosa* extract in rats'. *Phytomedicine* **2002**, *9*, 739–742. [CrossRef]
28. Ahmed, S.; Sultana, M.; Mohtasheem Ul Hasan, M.; Azhar, I. Analgesic and antiemetic activity of *Cleome viscosa*. *Pak. J. Bot.* **2011**, *43*, 119–122.
29. Wake Rajesh, R.; Patil Narhari, A.; Khadabadi, S.S. In vitro antibacterial activity of extracts of seeds of *Cleome viscosa* linn. *Int. J. Pharm. Sci. Rev. Res.* **2011**, *2*, 2232–2236.
30. Panduraju, T.; Parvathi, B.; Rammohan, M.; Srinivas Reddy, C. Wound healing property of *Cleome viscosa* linn. *Hygeia J. D Med.* **2011**, *3*, 41–45.
31. Mobiya, A.K.; Patidar, A.K.; Selvam, G.; Jeyakandan, M. Hepatoprotective effect of *Cleome viscosa* L. seeds in paracetamol induced hepatotoxic rats. *Int. J. Pharm. Biol. Arch.* **2010**, *1*, 399–403.
32. Bawankule, D.U.; Chattopadhyay, S.K.; Pal, A.; Saxena, K.; Yadav, S.; Faridi, U.; Darokar, M.P.; Gupta, A.K.; Khanuja, S.P. Modulation of inflammatory mediators coumarinolignoids from *Cleome viscosa* in female Swiss albino mice. *Inflammopharmacology* **2008**, *16*, 272–277. [CrossRef] [PubMed]
33. Rajani, A.; Sunitha, E.M.; Shailaja, K. Analysis of phytochemical constituents in leaf extract of *Cleome viscosa*. *World J. Pharm. Res.* **2014**, *3*, 1008–1013.
34. Mishra, A.; Mishra, A.K.; Jain, S.K. Anticonvulsant activity of *Cleome viscosa* seed extracts in Swiss albino mice. *Int. J. Pharm. Pharm. Sci.* **2010**, *2*, 177–181.
35. Sun, Y.; Xia, Y. Shape-controlled synthesis of gold and silver nanoparticles. *Science* **2002**, *298*, 2176–2179. [CrossRef]
36. Brindha, P.; Niraimathi, K.L.; Karunanithi, M. Phytochemical and in vitro screening of aerial parts of *Cleome viscosa* Linn. extracts (Capparidaceae). *Int. J. Pharm. Pharm. Sci.* **2012**, *4*, 27.
37. Mittal, A.K.; Kaler, A.; Banerjee, U.C. Free radical scavenging and antioxidant activity of silver nanoparticles synthesized from flower extract of *Rhododendron dauricum*. *Nano Biomed. Eng.* **2012**, *4*, 118–124. [CrossRef]
38. Nayak, D.; Pradhan, S.; Ashe, S.; Rauta, P.R.; Nayak, B. Biologically synthesized silver nanoparticles from three diverse family of plant extracts and their anticancer activity against epidermoid A431 carcinoma. *J. Colloid Interface Sci.* **2015**, *457*, 329–338. [CrossRef]
39. Rajkuberan, C.; Sathishkumar, G.; Prabukumar, S.; Ravindran, K.; Wilson, A.; Sivaramakrishnan, S. Formulation of *Carica papaya* latex-functionalized silver nanoparticles for its improved antibacterial and anticancer applications. *J. Mol. Liquids* **2016**, *219*, 232–238.
40. Rajkuberan, C.; Prabukumar, S.; Sathishkumar, G.; Wilson, A.; Ravindran, K.; Sivaramakrishnan, S. Facile synthesis of silver nanoparticles using *Euphorbia antiquorum* L. latex extract and evaluation of their biomedical perspectives as anticancer agents. *J. Saudi Chem. Soc.* **2017**, *21*, 911–919. [CrossRef]
41. Calandra, P. Synthesis of Ni nanoparticles by reduction of $NiCl_2$ ionic clusters in the confined space of AOT reversed micelles. *Mater. Let.* **2009**, *63*, 2416–2418. [CrossRef]
42. Longoa, A.; Calandrab, P.; Casalettoa, M.P.; Giordanob, C.; Veneziaa, A.M.; Turco Liverib, V. Synthesis and physico-chemical characterization of gold nanoparticles softly coated by AOT. *Mater. Chem. Phys.* **2006**, *96*, 66–72. [CrossRef]
43. Balashanmugam, P.; Prabhu, D.; Balakumaran, M.D.; Kalaichelvan, P.T. Phytosynthesized gold nanoparticles from *C. roxburghii* DC. leaf and their toxic effects on normal and cancer cell lines. *J. Photochem. Photobiol.* **2016**, *165*, 163–173. [CrossRef] [PubMed]
44. Sudha, A.; Jeyakanthan, J.; Srinivasan, P. Green synthesis of silver nanoparticles using *Lippia nodiflora* aerial extract and evaluation of their antioxidant, antibacterial and cytotoxic effects. *Resour. Effic. Technol.* **2017**, *3*, 506–515. [CrossRef]
45. Thirunavoukkarasu, M.; Balaji, U.; Behera, S.; Panda, P.K.; Mishra, B.K. Biosynthesis of silver nanoparticle from leaf extract of *Desmodium gangeticum* (L.) DC. and its biomedical potential. *Spectrochim. Acta A* **2013**, *116*, 424–427. [CrossRef]
46. Patra, S.; Mukherjee, S.; KumarBarui, A.; Ganguly, A.; Sreedhar, B.; Patra, C.R. Green synthesis, characterization of gold and silver nanoparticles and their potential application for cancer therapeutics. *Mater. Sci. Eng. C Mater. Biol. Appl.* **2015**, *53*, 298–309. [CrossRef]

47. El-Nour, K.M.M.A.; Eftaiha, A.; Al-Warthan, A.; Ammar, R.A.A. Synthesis and applications of silver nanoparticles. *Arab. J. Chem.* **2010**, *3*, 135–140. [CrossRef]
48. Lee, S.H.; Jun, B.H. Silver nanoparticles: Synthesis and application for nanomedicine. *Int. J. Mol. Sci.* **2019**, *20*, 865. [CrossRef]
49. Raja, S.; Ramesh, V.; Thivaharan, V. Green bio synthesis of silver nanoparticles using *Calliandra haematocephala* leaf extract, their antibacterial activity and hydrogen peroxide sensing capability. *Arab. J. Chem.* **2017**, *10*, 253–261. [CrossRef]
50. Mohanpuria, P.; Rana, N.K.; Yadav, S.K. Biosynthesis of nanoparticles: Technological concepts and future applications. *J. Nanopart. Res.* **2008**, *10*, 507–517. [CrossRef]
51. Hamouda, R.A.; Hussein, M.H.; Abo-elmagd, R.A.; Bawazir, S.S. Synthesis and biological characterization of silver nanoparticles derived from the cyanobacterium *Oscillatoria limnetica*. *Sci. Rep.* **2019**, *9*, 13071. [CrossRef] [PubMed]
52. Prabhu, D.; Arulvasu, C.; Babu, G.; Manikandan, R.; Srinivasan, P. Biologically synthesized green silver nanoparticles from leaf extract of *Vitex negundo* L. induce growth-inhibitory effect on human colon cancer cell line HCT15. *Process Biochem.* **2013**, *48*, 317–324. [CrossRef]
53. Babu, G.; Arulvasu, C.; Prabhu, D.; Jegadeesh, R.; Manikandan, R. Biosynthesis and characterization of silver nanoparticles from *Datura inoxia* and its apoptotic effect on human breast cancer cell line MCF7. *Mater. Lett.* **2014**, *122*, 98–102.
54. Bhattacharya, R.; Murkherjee, P. Biological properties of naked metal nanoparticles. *Adv. Drug Deliv. Rev.* **2008**, *60*, 1289–1306. [CrossRef]
55. Ramalingam, B.; Parandhaman, T.; Das, S.K. Antibacterial effects of biosynthesized silver nanoparticles on surface ultrastructure and nanomechanical properties of gram negative bacteria viz. *Escherichia coli* and *Pseudomonas aeruginosa*. *ACS Appl. Mater. Interfaces* **2016**, *8*, 4963–4976. [CrossRef]
56. Parida, U.K.; Biswal, S.K.; Bindhani, B.K. Green synthesis and characterization of gold nanoparticles: Study of its biological mechanism in human SUDHL-4 cell line. *Adv. Biol. Chem.* **2014**, *4*, 360–375. [CrossRef]
57. Harishkumar, S.; Satyanarayan, N.D.; Santhosha, S.M. Antiproliferative and in silico ADMET study of new 4-(piperidin-1-ylmethyl)-2- (thiophen-2-yl) quinoline analogues. *Asian J. Pharm. Clin. Res.* **2018**, *11*, 306–313.
58. Harishkumar, S.; Satyanarayan, N.D.; Raghavendra, R.; Nandini, H.S.; Prabhudas, N.; Kiranmayee, P. Cytotoxicity evaluation and in silico ADMET study of new (E)-1-(4-chlorobenzyl)-N'-benzylidene-5-bromo-1h-indole-2-carbohydrazides. *Der. Pharma Chem.* **2018**, *10*, 49–56.
59. Patil, M.P.; Kim, G.D. Eco-friendly approach for nanoparticles synthesis and mechanism behind antibacterial activity of silver and anticancer activity of gold nanoparticles. *Appl. Microbiol. Biotechnol.* **2017**, *101*, 79–92. [CrossRef]
60. Kanagamani, K.; Muthukrishnan, P.; Shankar, K.; Kathiresan, A.; Barabadi, H.; Saravanan, M. Antimicrobial, cytotoxicity and photocatalytic degradation of norfloxacin using *Kleinia grandiflora* mediated silver nanoparticles. *J. Clust. Sci.* **2019**, *30*, 1415–1424. [CrossRef]
61. Sarkar, S.; Kotteeswaran, V. Green synthesis of silver nanoparticles from aqueous leaf extract of Pomegranate (*Punica granatum*) and their anticancer activity on human cervical cancer cell. *Adv. Nat. Sci. Nanosci. Nanotechnol.* **2018**, *9*, 025014. [CrossRef]
62. Degterev, A.; Boyce, M.; Yuan, J. A decade of caspases. *Oncogene* **2003**, *22*, 8543–8567. [CrossRef] [PubMed]
63. Jayaraj, M.; Arun, R.; Sathishkumar, G.; MubarakAli, D.; Rajesh, M.; Sivanandhan, G.; Kapildev, G.; Manickavasagam, M.; Thajuddin, N.; Ganapathi, A. An evidence on G2/M arrest, DNA damage and caspase mediated apoptotic effect of biosynthesized gold nanoparticles on human cervical carcinoma cells (HeLa). *Mater. Res. Bull.* **2014**, *52*, 15–24. [CrossRef]
64. Ruchko, M.; Gorodnya, O.; LeDoux, S.P.; Alexeyev, M.F.; Al-Mehdi, A.B.; Gillespie, M.N. Mitochondrial DNA damage triggers mitochondrial dysfunction and apoptosis in oxidant challenged lung endothelial cells. *Am. J Physiol. Lung Cell. Mol. Physiol.* **2005**, *288*, 530–535. [CrossRef]
65. Manikandan, R.; Beulaja, M.; Prabhu, N.M.; Thiagarajan, R.; Anjugam, M.; Palanisamy, S.; Saravanan, K.; Arumugam, M. Synthesis of silver nanoparticles using *Solanum trilobatum* fruits extract and its antibacterial, cytotoxic activity against human breast cancer cell line MCF7. *Spectrochim. Acta A Mol. Biomol. Spectrosc.* **2015**, *5*, 223–228.

66. De Matteis, V.; Malvindi, M.A.; Galeone, A.; Brunetti, V.; De Luca, E.; Kote, S.; Kshirsagar, P.; Sabella, S.; Bardi, G.; Pompa, P.P. Negligible particle-specific toxicity mechanism of silver nanoparticles: The role of Ag^+ ion release in the cytosol. *Nanomed. Nanotechnol. Biol. Med.* **2015**, *11*, 731–739. [CrossRef]
67. Yeasmin, S.; Malik, D.; Das, T.; Bandyopadhyay, A. Green synthesis of silver nano/micro particles using TKP and PVA and their anticancer activity. *RSC Adv.* **2015**, *5*, 39992–39999. [CrossRef]
68. Awasthi, K.K.; Awasthi, A.; Verma, R.; Kumar, N.; Roy, P.; Awasthi, K.; John, P. Cytotoxicity, genotoxicity and alteration of cellular antioxidant enzymes in silver nanoparticles exposed CHO cells. *RSC Adv.* **2015**, *5*, 34927–34935. [CrossRef]
69. Guo, D.; Zhu, L.; Huang, Z.; Zhou, H.; Ge, Y.; Ma, W.; Wu, J.; Zhang, X.; Zhou, X.; Zhang, Y.; et al. Anti-leukemia activity of PVP-coated silver nanoparticles via generation of reactive oxygen species and release of silver ions. *Biomaterials* **2013**, *34*, 7884–7894. [CrossRef]
70. Mossman, T. Rapid colorimetric assay for cellular growth and survival: Application to proliferation and cytotoxicity assays. *J. Immun. Methods* **1983**, *65*, 55–63. [CrossRef]
71. Prabhu, D.; Arulvasu, C.; Babu, G.; Manikandan, R.; Srinivasan, P.; Govindaraju, K.; Ashokkumar, T. Synthesis and characterization of silver nanoparticles using crystal compound of sodium para-hydroxybenzoate tetrahydrate isolated from *Vitex negundo*. L leaves and its apoptotic effect on human colon cancer cell lines. *Eur. J. Med. Chem.* **2014**, *84*, 90–99.